Am J Transl Res 2026;18(5):4290-4304
www.ajtr.org /ISSN:1943-8141/AJTR0172666

Original Article

GM-CSF and IL-1α secreted by cryopreserved porcine skin promote angiogenesis in burn wounds by activating the JAK2/STAT3 pathway

Yuxing Liu, Haibin Zuo, Yang Shao, Cong Gao, Xinzhuang Liu, Guodong Song

Departments of Burns and Plastic Surgery & Wound Repair, Jinan Central Hospital, Shandong University, Jinan 250013, Shandong, China

Received March 16, 2026; Accepted May 13, 2026; Epub May 15, 2026; Published May 30, 2026

Abstract: Objective: Cryopreserved porcine skin (CPS) is widely applied in skin grafting for burns. In this study, we aimed to investigate the effects and underlying mechanisms of CPS on burn wound healing. Methods: Cryopreserved porcine skins were acquired. Guinea pig burn models were established and grafted with thawed-CPS. Human umbilical vein endothelial cells (HUVECs) were cultured in CPS-conditioned medium. Histological structure was assessed by hematoxylin-eosin (HE) staining. Protein levels were detected using enzyme-linked immunosorbent assay (ELISA), western blot, and immunohistochemistry. HUVECs proliferation was evaluated by 5-ethynyl-2'-deoxyuridine (EdU) assay. The invasion and migration of HUVECs were analyzed via Transwell assay. Tube formation was also assessed. Results: CPS maintained its structural integrity and cellular viability, with lower antigenicity compared with fresh porcine skin. Granulocyte-macrophage colony-stimulating factor (GM-CSF) and interleukin-1 alpha (IL-1α) secreted by CPS were detected in the CPS-grafted burned tissue. Moreover, CPS grafting accelerated wound healing and angiogenesis in burned guinea pigs. In vitro, CPS-conditioned medium enhanced the proliferation, invasion, migration, and tube formation of HUVECs, as well as activated the JAK2/STAT3 pathway. Neutralizing antibodies against GM-CSF and IL-1α synergistically reversed the pro-angiogenic effects of CPS in vivo and in vitro. Additionally, JAK2 inhibitor AG490 abolished the enhanced proliferation, invasion, migration, and tube formation of HUVECs induced by CPS-conditioned medium. Conclusion: We confirmed that CPS-secreted GM-CSF and IL-1α promoted angiogenesis in burn tissue by activating the JAK2/STAT3 pathway, thereby revealing an active therapeutic role of CPS for burn wound healing and offering theoretical support for its clinical application.

Keywords: Cryopreserved porcine skin, angiogenesis, burn wound healing, the JAK2/STAT3 pathway, GM-CSF, IL-1α

Introduction

Burn injury is among the most complex and devastating forms of physical trauma [1]. Except for the pain of treatment, extensive burns leave patients with both physical scars and psychological trauma [2]. The skin defect of burns can lead to numerous systemic complications, such as shock, severe water and electrolyte imbalances, visceral complications, burn wound infection, and multiple organ dysfunction [3]. Skin grafting to close the wound is the most effective treatment approach, and autologous skin is the most suitable material for covering burn wounds [3]. Autologous skin offers excellent adhesion and is non-immunogenic, thus avoiding immune rejection. However, the application of autologous skin grafting is often severely limited by the insufficient availability of donor skin [4]. Therefore, xenogeneic skin-based biological dressings are considered a primary direction for covering burn wounds.

Due to its histological structure and functions, such as adhesion, breathability, and collagen structure and content, porcine skin is similar to human skin, and it is easily obtainable [5]. Porcine skin becomes the primary source of xenogeneic skin, widely used in the clinical treatment of burn wounds [5]. Porcine skin can provide a moist, slightly acidic biological barrier environment for the wound, which reduces the

https://doi.org/10.62347/TMKD9184

risk of wound infection, induces the regeneration of tissue cells, and promotes wound healing [6]. After the wound has healed, the porcine skin sloughs off naturally, which significantly reduces the frequency of dressing changes compared to traditional non-biological dressings and effectively improves patient comfort [5]. Besides, Armato et al. found that, compared to fresh porcine skin, the tissue structure of cryopreserved porcine skin remained intact after thawing [7]. Furthermore, freezing can alter the antigenic determinants on proteins of the cell membrane surface and reduce the number of Langerhans cells, thereby lowering their antigenicity [8]. Cryopreserved porcine skin (CPS) was successfully transplanted onto burnt porcine individuals, with no difference in its effect on wound healing compared to fresh porcine skin [9]. CPS can meet the demands of treating extensive burns, especially in catastrophic or mass casualty incidents, providing diverse options for clinical practice [10, 11]. However, the mechanism by which CPS promotes wound healing in burns has not yet been studied.

Angiogenesis is a critical stage in wound healing, as it supplies oxygen and nutrients, removes metabolic waste to promote the proliferation and migration of epithelial cells, thereby facilitating wound closure [12]. Granulocyte-macrophage colony-stimulating factor (GM-CSF, also known as CSF2) is a monomeric glycoprotein produced by various cells, including macrophages, T cells, mast cells, natural killer cells, endothelial cells, and fibroblasts [13]. GM-CSF is involved in biological processes such as immune responses, cell differentiation and proliferation, and angiogenesis [13]. During wound healing, GM-CSF promoted angiogenesis through the Ang-1/Ang-2 system [14]. Parallelly, GM-CSF activated the JAK2/STAT3 pathway to promote angiogenesis by initiating the autophosphorylation of JAK2 in endothelial cells [15]. Additionally, Interleukin-1 alpha (IL-1α), a cytokine of the IL-1 family encoded by the IL1A gene, is primarily produced by macrophages, neutrophils, epithelial cells, and endothelial cells. It participates in various processes, including inflammation, cell proliferation, and angiogenesis [16]. Studies reported that IL-1α could induce the expression of pro-angiogenic cytokines, such as CXCL1, in brain endothelial cells to promote endothelial cell proliferation, migration, and angiogenesis in ischemic brain injury [16, 17]. Concurrently, IL-1α can promote the activation of the JAK2/STAT3 pathway [18]. It was revealed that JAK2/STAT3 pathway activation could increase angiogenesis by promoting Vascular endothelial growth factor A (VEGFA) expression [19]. JAK2/STAT3 pathway activation can promote cyclin D1, c-Myc and MMP2/9 expressions to facilitate the proliferation and migration of endothelial cells [20, 21]. Furthermore, Armato et al. verified that CPS continuously secretes cytokines such as GM-CSF and IL-1α after transplantation, suggesting its potential to actively promote burn wound healing [7]. However, their study only characterized these secretory properties and did not elucidate the specific mechanisms by which CPS promotes burn wound healing. Given the critical role of angiogenesis in wound healing and the known pro-angiogenic functions of GM-CSF and IL-1α, it remains unexplored whether these specific cytokines secreted by CPS drive burn wound healing via angiogenesis.

In this study, we established guinea pig burn models and performed CPS xenografts. The levels of GM-CSF and IL-1α secreted by the grafted CPS, and their effects on burn wound healing and angiogenesis, were evaluated. Concurrently, human umbilical vein endothelial cells (HUVECs) were cultured in the conditioned medium of CPS to verify whether the GM-CSF and IL-1α secreted by CPS promoted angiogenesis through the JAK2/STAT3 signaling pathway.

Materials and methods

Cryopreserved porcine skin obtained

Male Yorkshire pigs (35-45 kg) were purchased from Xi'an Yifengda Biotechnology Co., Ltd. (Xi'an, China). Nucleic acid tests for African Swine Fever Virus and Foot-and-Mouth Disease Virus were both negative (Test Report No: HRJC-WT-202203359). The experiments involving pigs were approved by the Experimental Animal Management and Ethics Committee of Jinan Central Hospital (approval number: JNCHIACUC2022-35; approval date: April 13, 2022). The pigs showed no obvious skin lesions or injuries. After the pigs were euthanized by intravenous injection of pentobarbital sodium (150 mg/kg, Sigma-Aldrich, USA) [22], the

body surface was first shaved, scrubbed with soapy water, and rinsed with clean water. The full-thickness skin, along with part or all of the underlying subcutaneous tissue, was harvested along the cervico-scapulo-withers. Residual long hairs were then shaved off, the edges of the skin tissue were trimmed, and the skin tissues were subsequently washed 3 times with clean water, soaked in 0.05% chlorhexidine solution (Sinopharm, China) for 15 min, and rinsed with isotonic saline (Solarbio, China) 3 times following immersion in RPMI 1640 medium (Gibco, USA). Under aseptic conditions, the skin tissue was processed into 0.4-0.5 mm thick skin tissues and was placed into cryoprotectant solution (10% DMSO (Sigma-Aldrich, USA) + 10% glycerol (Sigma-Aldrich, USA) + 0.5 mol/L trehalose (Sigma-Aldrich, USA) + RPMI 1640) sequentially at 4°C for 1.5 h, -25°C for 2 h, -78°C for 10 h, and then stored long-term at -150°C. For thawing, the CPS was quickly placed into a 42°C constant temperature water bath (Julabo, Germany) containing isotonic saline and stirred continuously. After the skin tissues softened (thawed to 0-4°C), they were washed with 4°C isotonic saline 3 times and cultured in RPMI 1640 medium [7].

Hematoxylin-eosin (HE) staining and transmission electron microscope (TEM) examination

After deparaffinization and rehydration with xylene (Sinopharm, China) and gradient concentration alcohol (Sinopharm, China), porcine skin tissue sections or guinea pig burn tissue sections were stained using hematoxylin (Beyotime, China) for 10 min and eosin (Beyotime, China) for 3 min. The sections were dehydrated and cleared following observation under a microscope (CX23, Olympus, Japan).

The submicroscopic structure of the CPS tissue was examined using TEM (Hitachi, Japan).

Antigen detection assay

Fresh porcine skin and thawed CPS were minced and placed in normal saline for 48 h at 4°C. Subsequently, glass powder (Solarbio, China) was added, and the porcine skin tissues were ground into homogenate and centrifuged at 3,000 r/min for 10 min. The supernatant was collected to determine the antigenic protein content. For the preparation of immune sera in the two groups, guinea pigs were injected three times with the antigenic protein of fresh and cryopreserved porcine skin. Each guinea pig received 2 mg of antigenic protein per injection. For the first immunization, antigen dissolved in complete Freund's adjuvant (Beyotime, China) was administered into the footpads and groin of guinea pigs. The subsequent two injections, in which the antigen was dissolved in incomplete Freund's adjuvant, were given as multiple subcutaneous injections in the abdominal and axillary regions. The second immunization was performed 3 weeks after the first, and the third immunization was performed 10 days later. Ten days after the final immunization, blood was collected from the vein of the guinea pigs. The levels of IgG and IgM were detected using the corresponding ELISA kit (#CSB-E10125Gu, CUSABIO, China; #JN21820, Jining Bio, China) [23].

Flow cytometric analysis

Porcine skin tissue homogenate was diluted with FACS buffer (BD Biosciences, USA). The swine leukocyte antigen (SLA) class I and SLA class II mAb (Abcam, USA) were used to culture the porcine cells, followed by FITC-conjugated mAb (Abcam, USA) staining. The fluorescence intensity was analyzed by flow cytometry (BD LSR II, BD Biosciences, USA) [24].

Burn model

Male guinea pigs (10 weeks, 300-400 g, n = 36) were purchased from Beijing Wealthy Experimental Animal Breeding Center (Beijing, China). The experiments involving guinea pigs were approved by the Ethics Committee of Institutional Animal Care and Use Committee of Contec Medical Testing Services Hebei Co., Ltd. (approval number: MDL-2025-3-55; approval date: March 15, 2025). The guinea pigs were fed a standard guinea pig diet supplemented with essential vitamins and provided with free access to water [25]. They were acclimatized for 5 days. Then, guinea pigs were anesthetized via intramuscular injection of 40-50 mg/kg ketamine and 4-5 mg/kg xylazine [26]. After shaving the guinea pigs' skin, two standardized deep second-degree burns were created on each side of the spine on the back of each guinea pig. A custom-made iron template was preheated to 75°C in water, then gently pressed against the skin with full contact for 5 seconds to induce a deep burn. The

burned guinea pigs were randomly divided into: burn group (model), burn + CPS graft group (CPS), burn + CPS graft + isotype control group (CPS + isotype), burn + CPS graft + GM-CSF neutralizing antibody group (CPS + anti-GM-CSF), burn + CPS graft + IL-1α neutralizing antibody group (CPS + anti-IL-1α), burn + CPS graft + GM-CSF and IL-1α neutralizing antibodies group (CPS + anti-GM-CSF-IL-1α). Except for the model group, burned guinea pigs in other groups received CPS graft. The CPS + anti-GM-CSF, CPS + anti-IL-1α, and CPS + anti-GM-CSF-IL-1α groups received daily intradermal injections of 57 μg/kg anti-GM-CSF (Specifically acts on pig, #PA5-48106, Invitrogen, USA) [27] and/or 1.7 μg/kg anti-IL-1α (Specifically acts on pig, #PA5-47876, Invitrogen, USA) [28] after CPS grafting. The CPS + isotype group received an equivalent dose of isotype control antibody. In the CPS group, porcine skin tissues were collected before grafting and at 5 and 10 days post-grafting to assess GM-CSF and IL-1α release levels. After CPS grafting for 10 days, the guinea pigs were euthanized CO_2 suffocated [29], and skin tissues from the burn area were harvested for analysis [25, 26]. Healing rate (%) = [(Initial wound area - Final wound area)/Initial wound area] × 100% [30].

Enzyme-linked immunosorbent assay (ELISA)

Thawed CPS and fresh porcine skin tissues were cut into 2.5 cm × 2.5 cm and cultured in RPMI 1640 containing 5% horse serum (#26050070, Gibco, USA) [7]. The level of alpha-Galactosidase A (α-Gal) antigen was analyzed using the ELISA Kit (#JLC9488-48T, Gelatins, China) [23]. The levels of GM-CSF and IL-1α were detected every three days. Additionally, burned tissues of guinea pigs were also analyzed for GM-CSF and IL-1α levels secreted by CPS. The levels of GM-CSF and IL-1α were detected using the porcine-specific ELISA Kits (#DY711, #DY680, R&D Systems, USA) according to the manufacturer's instructions.

Immunohistochemical (IHC) assay

Paraffin-embedded sections of CPS and burn tissue were deparaffinized in xylene and rehydrated through a graded ethanol series. Then, the sections were treated with Tris-EDTA for 5 min and H_2O_2 for 15 min. After blocking with 5% goat serum for 30 min, the sections were incubated with primary antibodies against GM-CSF (Specifically acts on pig, #PA5-48106, Invitrogen, USA), IL-1α (Specifically acts on pig, #PA5-47876, Invitrogen, USA), VEGFA (#PA1-16948, Invitrogen, USA), and CD31 (#sc-376764, Santa Cruz Biotechnology, USA) for 2.5 h, followed by incubation with donkey-anti secondary antibodies (#ab150129, Abcam, USA) for 30 minutes. 3,3'-Diaminobenzidine Tetrahydrochloride (DAB) (#P0203, Beyotime, China) was added for color development, and the sections were counterstained with Mayer's hematoxylin (#H3136, Sigma, USA). Finally, the sections were dehydrated, cleared, and observed under a microscope (CX23, Olympus, Japan).

Western blot

The burned tissues and HUVECs were lysed with lysis buffer (#9164, Takara, Japan) containing protease inhibitor, and total protein was extracted. After determining the concentration of protein using the Bicinchoninic Acid Kit (Sigma, USA), the protein was separated by sodium dodecyl sulfate-polyacrylamide gel electrophoresis and transferred onto PVDF membrane (#24937-79-9, Sigma, USA). BSA was applied to block the membranes for 1 h at room temperature. Then, the members were incubated with primary antibodies against VEGFA (#PA1-16948, Invitrogen, USA), p-JAK2 (#ab32101, Abcam, USA), JAK2 (#ab108596, Abcam, USA), p-STAT3 (#ab76315, Abcam, USA), STAT3 (#ab68153, Abcam, USA) and GAPDH (#ab8245, Abcam, USA) at 4°C overnight and donkey-anti secondary antibodies (#ab150129, Abcam, USA) for 2 h at room temperature. The bands were visualized with a chemiluminescent substrate in a chemiluminescence imaging system (#ChemiDoc, Bio-Rad, USA) and quantified with ImageJ software (version 1.52a).

Preparation of CPS-conditioned medium

According to our experimental protocol, after being washed three times with normal saline, the thawed CPS was soaked in RPMI 1640 medium supplemented with antibiotics and 5% adult horse serum (#26050070, Gibco, USA) [7], at an approximate area-to-volume ratio of 2 cm^2:1 ml. The samples were cultured at 37°C in a 5% CO_2 environment, with fresh

medium replaced every 3 days. We collected the conditioned medium on day 10 and centrifuged it to remove detached cell debris before using it for subsequent HUVEC experiments.

5-Ethynyl-2'-deoxyuridine (EdU) assay

HUVECs were seeded into 96-well plates with 5,000 cells/well and cultured in the conditioned medium of CPS, 1 μg/mL GM-CSF neutralizing antibody or/and 12 ng/mL IL-1α neutralizing antibody for 24 h. HUVECs were continuously incubated in 20 μM EdU for 2 h, followed by fixation with 4% paraformaldehyde (Beyotime, China) for 0.5 h and transparent with 0.5% Triton X-100 for 10 min. Reaction solution (50 μL) was added to every well for 0.5 h and DAPI was used to stain the nucleus for 5 min. The images were obtained under a fluorescence microscope (#Mateo FL, Leica, Germany).

Transwell assay

The invasion and migration of HUVECs were measured using a Transwell assay. HUVECs were planted into the Matrigel matrix (Corning, USA)-coated upper chamber to assess invasion ability, or into the uncoated upper chamber to evaluate migration ability, both supplied with serum-free DMEM medium (Gibco, USA). DMEM medium containing 10% fetal bovine serum (FBS, Gibco, USA) was added to the lower chamber. After 24 h of incubation, HUVECs were fixed with 4% polyformaldehyde (Beyotime, China) and stained with crystal violet (Beyotime, China). HUVECs that did not invade or migrate were removed and the result was observed using a microscope (CX23, Olympus, Japan).

Tube formation experiment

Melted Matrigel (10 μL, Corning, USA) was added to each well of a μ-Slide angiogenesis plate (IBIDI, Germany). After the gel solidified, 1×10^4 HUVECs were added to each well and cultured at 37°C for 6 h to observe tube formation.

Statistics

Data were tabulated and analyzed using GraphPad Prism version 8.0 software (GraphPad Software, USA) to calculate the mean and standard deviation (SD). All data are presented as mean ± SD. The unpaired t-test was used to compare differences between two groups, and one-way ANOVA followed by Tukey's post hoc test was applied for comparisons among multiple groups. *P* value of less than 0.05 was considered statistically significant.

Results

Cryopreserved porcine skin maintains intact structure and viability, and exhibits reduced antigenicity

HE staining revealed a clear demarcation between the epidermis and dermis, with dense fibrous tissue in the dermis and clearly visible hair follicle structures of fresh porcine skin. Aside from slight localized edema in the granular layer of the epidermis and the superficial dermis, the histomorphology of thawed CPS was well-preserved, showing no significant difference from the fresh porcine skin tissue (**Figure 1A**). The ultrastructure of fresh porcine skin and CPS was observed using TEM. The keratinocytes of fresh porcine skin had large nuclei, the basement membrane was continuous and intact, and the intercellular and cell-to-basement membrane connections were good. Fibroblasts were located beneath the basement membrane, and cell structure was intact, surrounded by a large amount of collagen fibers in fresh porcine skin tissues. In the thawed CPS, the keratinocytes exhibited swelling, and the intercellular and cell-to-basement membrane connections remained intact. The mitochondrial structure of the fibroblasts was undamaged, and a large number of collagen fibers surrounded them in thawed CPS. Compared with the fresh porcine skin, the overall structure of CPS remained intact and viable (**Figure 1B**). Moreover, flow cytometry and ELISA results showed that the levels of SLA class I and SLA class II, as well as α-Gal in CPS were decreased compared with fresh porcine skin, respectively (**Figure 1C**, **1D**). The levels of IgG and IgM in guinea pigs sensitized with cryopreserved skin were lower than those in guinea pigs sensitized with fresh skin (**Figure 1E**). Additionally, the ELISA result revealed that there was no significant difference in the secretion levels of GM-CSF and IL-1α between the CPS and fresh porcine skin

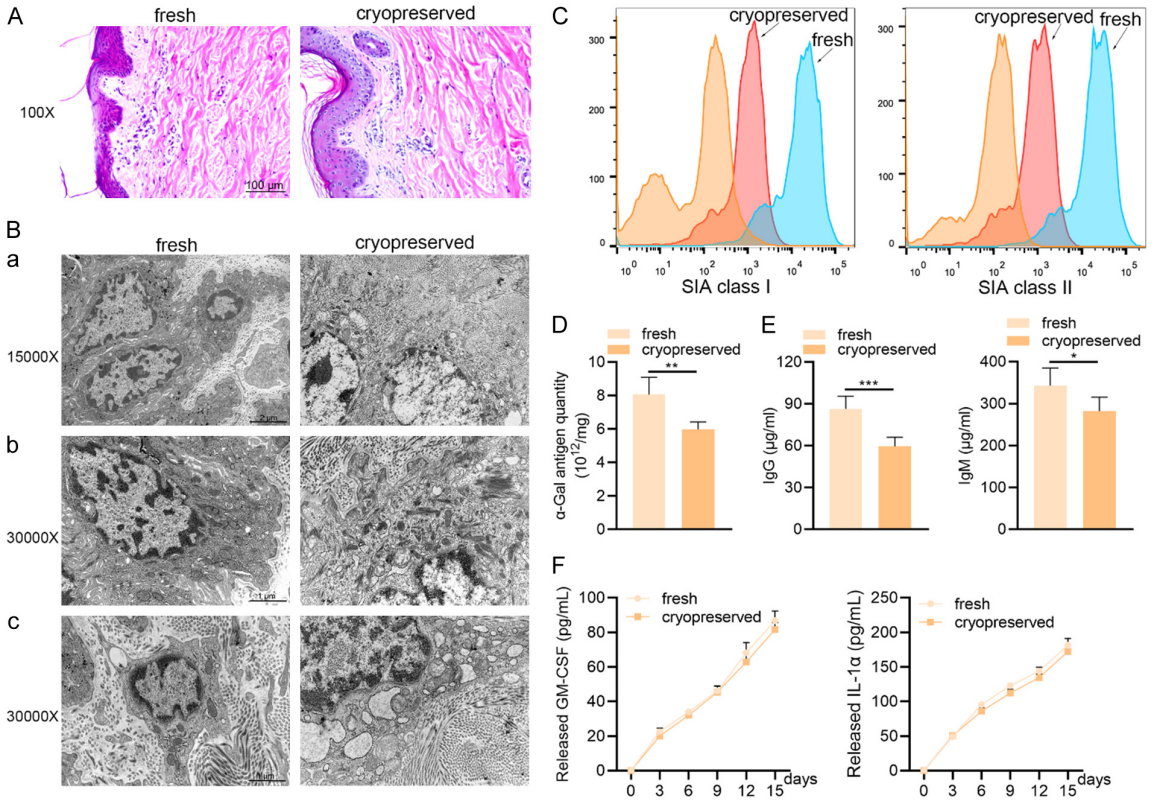

Figure 1. Cryopreserved porcine skin maintains cellular viability and exhibits reduced antigenicity. A. Hematoxylin-eosin (HE) staining was used to detect the structure of fresh porcine skin and CPS. Scale = 100 μm. B. Transmission electron microscope (TEM) was applied to observe the submicroscopic structure of fresh porcine skin and CPS. a. The junction between the epidermis and the dermis; b. keratinocyte; c. fibroblast. C. Swine leukocyte antigen (SLA) class I and SLA class II of CPS and fresh porcine skin were analyzed by flow cytometry. D. The level of alpha-Galactosidase A (α-Gal) antigen of CPS and fresh porcine skin was detected by enzyme-linked immunosorbent assay (ELISA). E. The levels of IgG and IgM of the guinea pig were assessed by ELISA. F. The levels of granulocyte-macrophage colony-stimulating factor (GM-CSF) and interleukin-1 alpha (IL-1α) secreted by cultured CPS were tested using ELISA. Data are presented as mean ± standard deviation (SD). $^{*}P < 0.05$, $^{**}P < 0.01$, $^{***}P < 0.001$.

(**Figure 1F**). Therefore, the results suggested that CPS maintained an intact structure and viability, and had lower antigenicity.

The secretion of GM-CSF and IL-1α from cryopreserved porcine skin enhances angiogenesis in the burned tissues of guinea pigs

To investigate the effect of CPS on the wound healing of burned skin, guinea pig burn models were constructed and transplanted with thawed CPS. The secretion levels of GM-CSF and IL-1α from the CPS after transplantation were assessed using IHC staining. No GM-CSF and IL-1α secretion was detected at transplantation day 0 with CPS. The secretion of GM-CSF and IL-1α was observed in CPS on day 5 and 10 after transplantation, with the levels of GM-CSF and IL-1α on day 10 being higher than those on day 5 (**Figure 2A**). After CPS grafting, the GM-CSF (specifically acts on pig, 57 μg/kg) and IL-1α (specifically acts on pig, 1.7 μg/kg) neutralizing antibodies were administered to the burn tissues. As shown in **Figure 2B**, **2C**, GM-CSF and IL-1α secreted by CPS were detected in the burned tissue post-CPS transplantation. GM-CSF and IL-1α neutralizing antibody administration weakened GM-CSF and IL-1α levels secreted by CPS (**Figure 2B**, **2C**). We monitored the changes in healing rate on days 0, 3, 5, 7, and 10, and presented the percentage of wound healing area on day 10. The results showed that compared with the model group, the wound healing rate in the CPS group was significantly increased on day 10. After treatment with GM-CSF or IL-1α neutralizing antibodies, the wound healing rate following

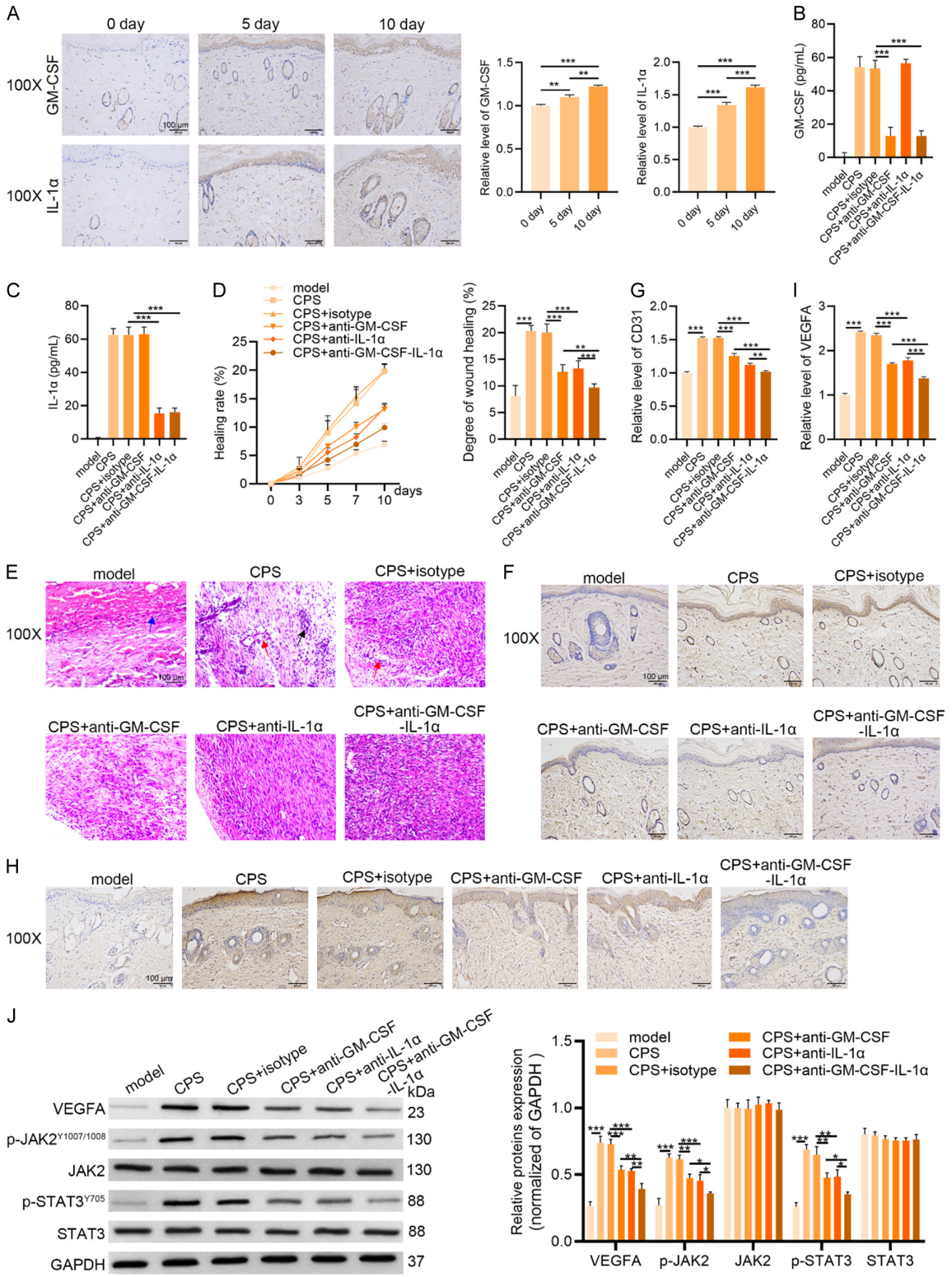

Figure 2. GM-CSF and IL-1α secreted by cryopreserved porcine skin facilitate angiogenesis in guinea pigs. (A) The secretion levels of GM-CSF and IL-1α were detected in CPS tissues using immunohistochemical (IHC) staining after CPS grafting. Scale = 100 μm. (B, C) The secretion levels of GM-CSF and IL-1α from CPS were assessed by ELISA assay in the burn tissues. (D) The wound healing rate was measured on days 0, 3, 5, 7, and 10, with the percentage of wound healing area presented on day 10. (E) The burn tissues were observed by HE staining (Blue arrow: inflammatory cells, red arrow: new blood vessels, black arrow: new hair follicles). Scale = 100 μm. (F) IHC staining

of cluster of differentiation 31 (CD31) in burn tissues (Scale = 100 μm) and the quantitative analysis of relative CD31 expression (G). (H) IHC staining of Vascular endothelial growth factor A (VEGFA) in burn tissues (Scale = 100 μm) and the quantitative analysis of relative VEGFA expression (I). (J) The levels of VEGFA, p-JAK2 and p-STAT3 were assessed via western blot in the burn tissues. Data are presented as mean ± SD. $^{*}P < 0.05$, $^{**}P < 0.01$, $^{***}P < 0.001$.

CPS transplantation was reduced; treatment with both neutralizing antibodies further decreased the wound healing rate (**Figure 2D**). HE staining revealed that in the model group, the burned tissue exhibited fewer newly formed blood vessels and less regeneration of dermal and hair follicles, accompanied by a massive infiltration of inflammatory cells. Following CPS transplantation, there was an increase in neovascularization, a denser distribution of collagen fibers, and significant regeneration of dermal and hair follicles. However, treatment with neutralizing antibodies against either GM-CSF or IL-1α attenuated the improvement effects of CPS transplantation on the burned tissue. When treated with neutralizing antibodies against both GM-CSF and IL-1α, the improvement effects of CPS transplantation were further diminished (**Figure 2E**). In addition, the IHC result revealed that CPS transplantation increased the endothelial cell marker CD31 and vascular formation regulatory factor VEGFA levels in burned tissue, and GM-CSF and IL-1α neutralizing antibodies reduced CD31 and VEGFA levels in burned tissue grafted with CPS. The levels of CD31 and VEGFA were decreased in the CPS + anti-GM-CSF-IL-1α group compared with the CPS + anti-GM-CSF and CPS + anti-IL-1α groups (**Figure 2F-I**). Likewise, the western blot result of VEGFA expression was consistent with that of the IHC staining. It was reported that GM-CSF and IL-1α could activate the JAK2/STAT3 pathway which contributed to angiogenesis [15, 18]. The levels of p-JAK2 and p-STAT3 were elevated in the CPS group compared with the model group, and GM-CSF and IL-1α neutralizing antibodies decreased the levels of p-JAK2 and p-STAT3 in the CPS + anti-GM-CSF and CPS + anti-IL-1α groups. Furthermore, the combination of neutralizing antibodies against GM-CSF and IL-1α reduced p-JAK2 and p-STAT3 levels to a greater extent than either neutralizing antibody alone (**Figure 2J**). According to these data, GM-CSF and IL-1α secreted by CPS synergistically enhanced angiogenesis and wound healing, as well as activated the JAK2/STAT3 pathway in burned guinea pigs.

GM-CSF and IL-1α secreted by cryopreserved porcine skin promote the proliferation, migration, and tube formation of HUVECs

To further investigate the mechanism of GM-CSF and IL-1α secreted by CPS on angiogenesis, HUVECs were cultured in CPS-conditioned medium with or without the neutralizing antibody against GM-CSF (specifically acts on pig, 1 μg/mL) and IL-1α (specifically acts on pig, 12 ng/mL). EdU assay was applied to assess the proliferation, and the invasion and migration abilities were detected by Transwell assay in CPS-conditioned medium, GM-CSF and IL-1α neutralizing antibodies-treated HUVECs. The tube formation of HUVECs was evaluated by the tube formation assay. The results displayed that the CPS-conditioned medium promoted the proliferation, invasion, migration, and tube formation of HUVECs. The pro-angiogenic effects of CPS-conditioned medium were inhibited by neutralizing antibodies against either GM-CSF or IL-1α and were further diminished upon their combined application (**Figure 3A-D**). These results verified that GM-CSF and IL-1α secreted by CPS acted synergistically to promote the proliferation, invasion, migration, and tube formation of HUVECs.

Additionally, treatment with CPS-conditioned medium upregulated VEGFA expression and enhanced the phosphorylation levels of JAK2 and STAT3 in HUVECs. Neutralizing antibody against GM-CSF or IL-1α attenuated VEGFA expression and p-JAK2 and p-STAT3 levels, a more pronounced reduction was found when neutralizing antibodies against GM-CSF and IL-1α were used in combination (**Figure 3E**). Together, these results indicated that GM-CSF and IL-1α secreted by CPS synergistically accelerated the proliferation, invasion, migration, and tube formation of HUVECs.

JAK2/STAT3 pathway mediates GM-CSF and IL-1α secreted by CPS-enhanced angiogenesis of HUVECs

Whether the JAK2/STAT3 pathway contributed to the proliferation, migration, and tube forma-

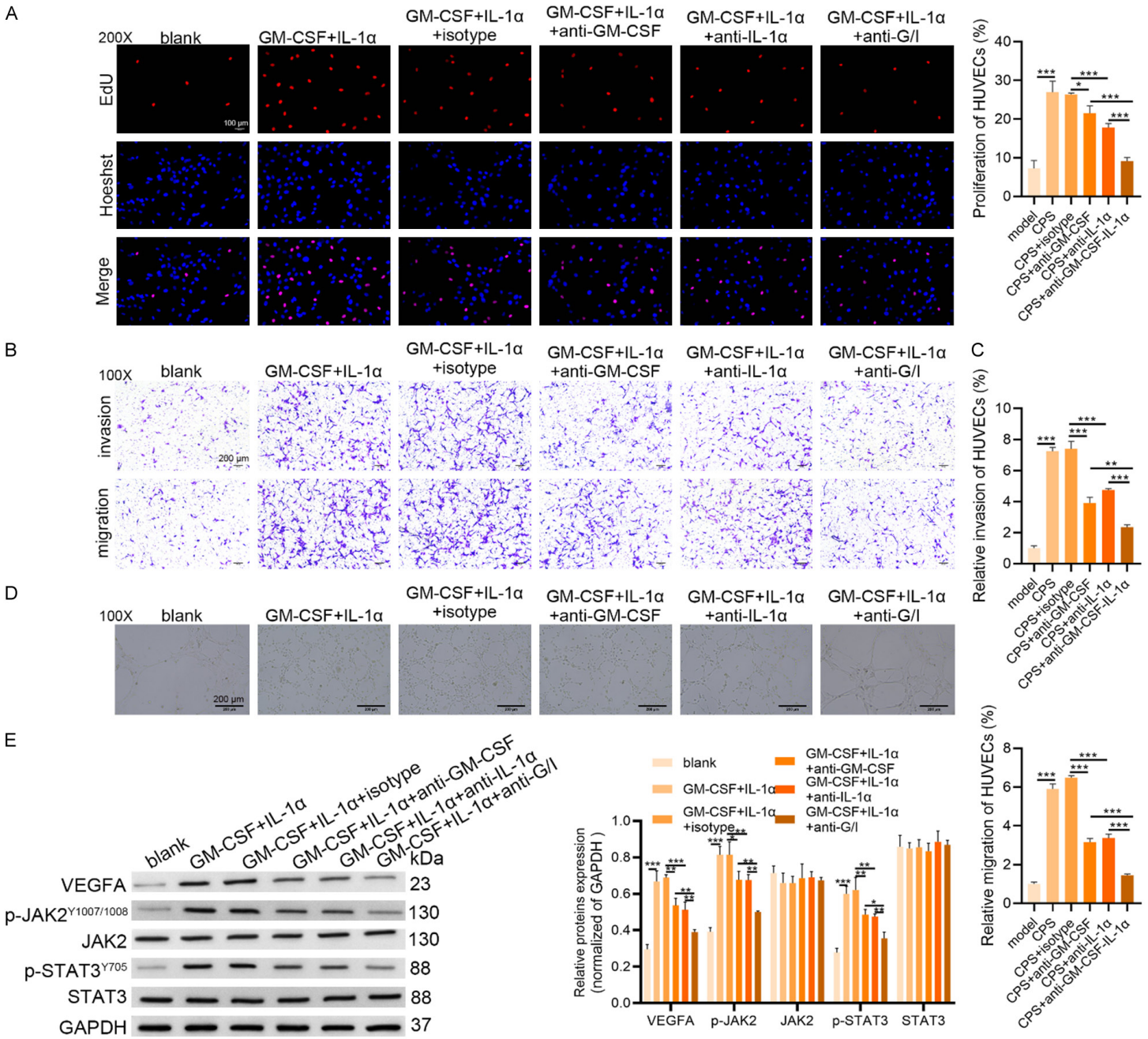
A
200X
blank
GM-CSF+IL-1α
GM-CSF+IL-1α +isotype
GM-CSF+IL-1α +anti-GM-CSF
GM-CSF+IL-1α +anti-IL-1α
GM-CSF+IL-1α +anti-G/I
EdU
Hoeshst
Merge
100 μm
Proliferation of HUVECs (%)
model
CPS
CPS+isotype
CPS+anti-GM-CSF
CPS+anti-IL-1α
CPS+anti-GM-CSF-IL-1α
B
100X
invasion
migration
200 μm
C
Relative invasion of HUVECs (%)
D
100X
200 μm
E
blank
GM-CSF+IL-1α
GM-CSF+IL-1α+isotype
GM-CSF+IL-1α+anti-GM-CSF
GM-CSF+IL-1α+anti-IL-1α
GM-CSF+IL-1α+anti-G/I
kDa
VEGFA 23
p-JAK2Y1007/1008 130
JAK2 130
p-STAT3Y705 88
STAT3 88
GAPDH 37
Relative proteins expression (normalized of GAPDH)
VEGFA
p-JAK2
JAK2
p-STAT3
STAT3
Relative migration of HUVECs (%)

Figure 3. CPS secretes GM-CSF and IL-1α to enhance the proliferation, migration, and tube formation of HUVECs. A. The proliferation of HUVECs was detected using EdU staining. Scale = 100 μm. B. The invasion and migration of HUVECs were assessed by Transwell assay. Scale = 200 μm. C. Quantification of the invasion and migration abilities of HUVECs. D. The tube formation was analyzed after HUVECs were treated with CPS-conditioned medium. Scale = 200 μm. E. The levels of VEGFA, p-JAK2 and p-STAT3 were assessed by western blot in CPS-conditioned medium-treated HUVECs. Data are presented as mean ± SD. *P < 0.05, **P < 0.01, ***P < 0.001. GM-CSF + IL-1α + anti-G/I: GM-CSF + IL-1α + anti-GM-CSF/IL-1α.

tion of HUVECs induced by GM-CSF and IL-1α secreted by CPS was explored. Before the addition of CPS-conditioned medium, HUVECs were pre-treated with the JAK2 inhibitor AG490 (10 μM) for 4 hours. CPS-conditioned medium treatment facilitated the proliferation, invasion, and migration of HUVECs, which were reversed by AG490 (**Figure 4A-C**). Furthermore, AG490 reduced the tube formation of HUVECs enhanced by the CPS-conditioned medium (**Figure 4D**). Parallelly, the CPS-conditioned medium upregulated the expression of VEGFA in HUVECs, and AG490 treatment decreased VEGFA expression in CPS-conditioned medium-treated HUVECs (**Figure 4E**). Concurrently, AG490 reduced the CPS-conditioned medium-induced phosphorylation levels of JAK2 and STAT3 (**Figure 4E**). These results suggested that the GM-CSF and IL-1α secreted by CPS promoted the proliferation, migration, and tube formation of HUVECs by activating the JAK2/STAT3 signaling pathway.

Discussion

Skin grafting is a widely used approach for managing burn-induced skin loss. Nevertheless, autografting is limited by its constrained availability [4]. Allogeneic skin grafts are restricted by donor shortages and ethical issues [31]. Consequently, xenogeneic skin grafting has become the preferred treatment option. Because porcine skin is highly similar to human skin in sebaceous glands, hair follicles, and collagen composition, it can conform well to human wounds after transplantation, which provides a physical barrier function [5]. After a porcine skin graft, a protective layer is formed that prevents the loss of water, protein, and electrolytes from the wound. It effectively isolates the wound from external bacteria, reducing the risk of infection, and covers exposed nerve endings to alleviate patient pain [4, 32]. For example, applying a porcine skin graft to the epidermal necrosis patient could reduce the patient's pain score [32]. However, when facing mass casualty burn events, obtaining large quantities of fresh porcine skin is time-consuming. Therefore, CPS becomes a very good choice. It was reported that thawed CPS was grafted to burn wounds in pigs to promote wound healing comparable to that achieved with fresh porcine skin [9]. In the present study, histological analysis revealed that while the dermal layer of the thawed CPS exhibited slight edema, its cellular architecture remained intact and viable, showing no significant differences from fresh porcine skin. Furthermore, the antigenicity of the thawed CPS was reduced compared with the fresh skin tissue, which was consistent with the results reported by Ju et al [8]. These findings indicated that CPS might elicit better clinical application effects compared with fresh porcine skin. Moreover, these structural and immunological advantages lay the foundation for its function not merely as a passive biological barrier, but potentially as an active participant in tissue repair.

Previously, porcine skin was regarded merely as a temporary dressing [33]. However, an increasing body of evidence suggests that porcine skin transplantation can promote wound regeneration and repair. For instance, porcine skin transplantation has been shown to increase the wound healing area [34]. Armato et al. found that cultured CPS secreted IL-1α, IL-6, GM-CSF, and TNF-α in vitro. Moreover, after the CPS was transplanted onto the wound of burn patients, the expression levels of IL-1α and GM-CSF secreted by grafted CPS on day 7 were significantly higher than on day 3 [7]. These cytokines play roles in processes such as inflammation, cell proliferation, and angiogenesis [17, 35]. In this study, we demonstrated that GM-CSF and IL-1α secreted by CPS released into the wounds of burned guinea pigs after transplanting CPS, which acted on the burn tissue to promote wound healing and angiogenesis. Concurrently, in vitro, GM-CSF and IL-1α secreted by CPS promoted the proliferation, migration and tube formation of HUVECs. When GM-CSF and IL-1α were neutralized using GM-CSF and IL-1α neutralizing

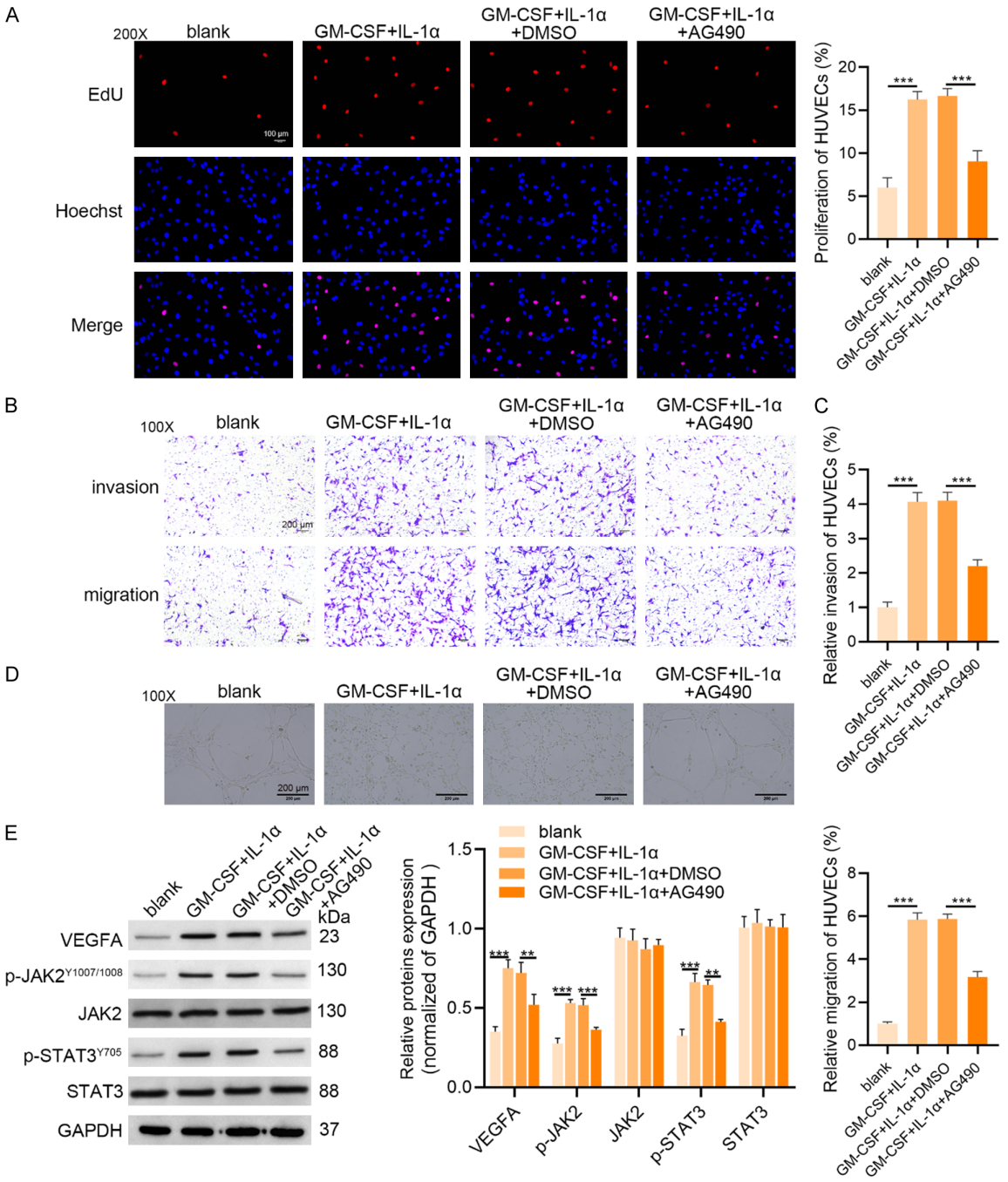

Figure 4. GM-CSF and IL-1α secreted by cryopreserved porcine skin accelerate the proliferation, migration, and tube formation of HUVECs via the JAK2/STAT3 pathway. A. The proliferation was tested using EdU staining in HUVECs treated with CPS-conditioned medium and JAK2 inhibitor AG490. Scale = 100 μm. B. The Transwell assay was performed to analyze the invasion and migration of CPS-conditioned medium and AG490-treated HUVECs. Scale = 200 μm. C. Quantification of the invasion and migration abilities of HUVECs. D. The tube formation was analyzed after HUVECs were treated with CPS-conditioned medium and AG490. Scale = 200 μm. E. Western bolt was employed to assess the levels of VEGFA, p-JAK2 and p-STAT3 in CPS-conditioned medium and AG490-treated HUVECs. Data are presented as mean ± SD. $^{**}P < 0.01$, $^{***}P < 0.001$. GM-CSF + IL-1α + anti-G/I: GM-CSF + IL-1α + anti-GM-CSF/IL-1α.

antibodies, the pro-angiogenic effect of the CPS was reversed, and the combination of the two neutralizing antibodies of GM-CSF and IL-1α was more effective than either alone.

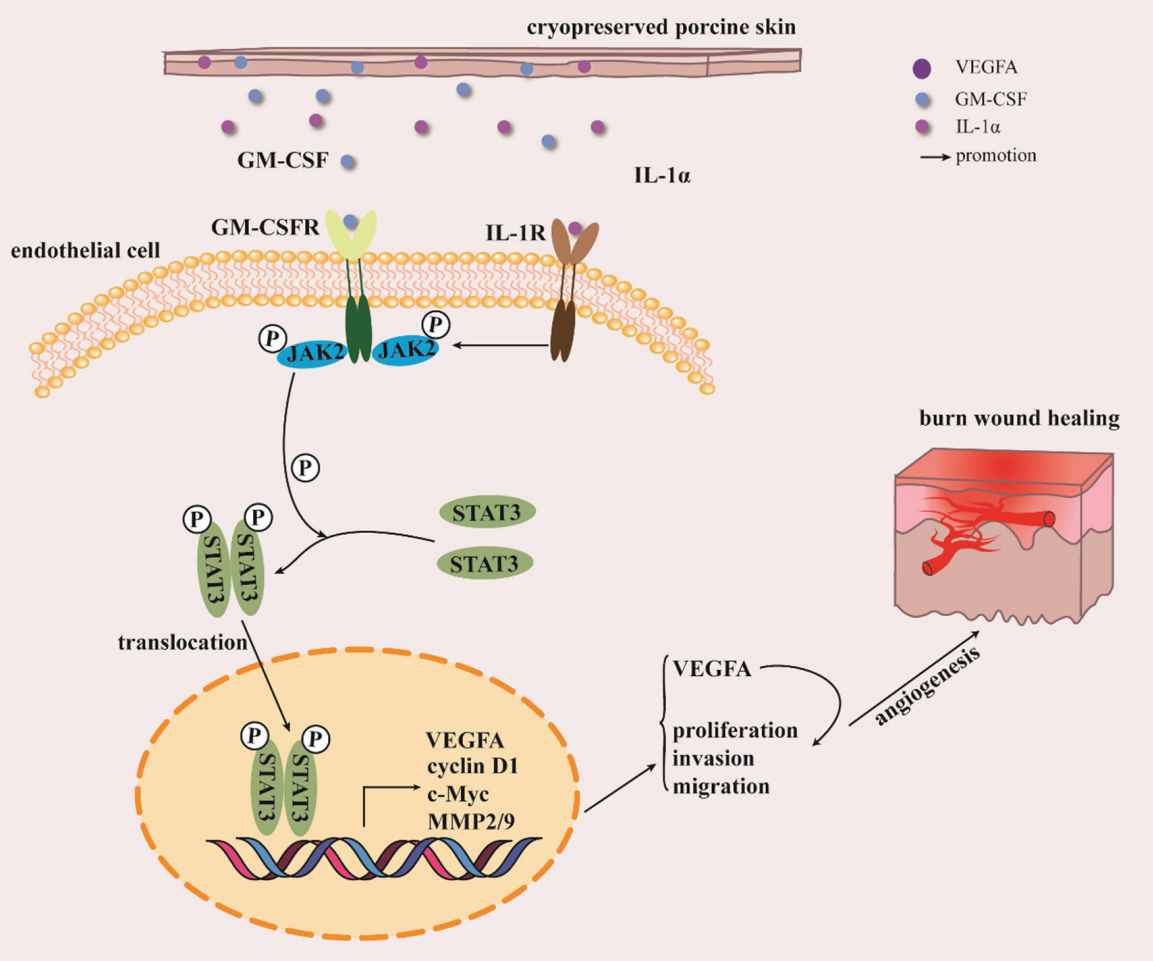

Figure 5. The graphical abstract demonstrates that cryopreserved porcine skin (CPS) promotes burn wound healing by secreting granulocyte-macrophage colony-stimulating factor (GM-CSF) and interleukin-1 alpha (IL-1α) to activate the JAK2/STAT3 pathway. Cryopreserved porcine skin secretes GM-CSF and IL-1α. GM-CSF and IL-1α bind to their receptor GM-CSFR and IL-1R to recruit and activate JAK2, respectively. Activated JAK2 undergoes autophosphorylation and phosphorylates STAT3. The phosphorylated STAT3 translocates into the nucleus to promote the expression of downstream genes, including Vascular endothelial growth factor A (VEGFA), which enhances the proliferation, invasion, and migration of endothelial cells, thereby promoting angiogenesis to facilitate burn wound healing.

These results indicate that GM-CSF and IL-1α secreted by CPS could synergistically promote angiogenesis of the burned wound. This synergistic effect is supported by a solid molecular basis: it has been reported that GM-CSF binds to its receptor GM-CSFR to initiate JAK2 phosphorylation in endothelial cells [15], while IL-1α binding to its receptor IL-1R can similarly promote the activation of the JAK2/STAT3 pathway [18]. Given that the activation of the JAK2/STAT3 pathway promotes angiogenesis [19], in the present study, GM-CSF and IL-1α act through their distinct upstream receptors and signaling cascades to converge and synergistically activate the JAK2/STAT3 pathway, thereby upregulating VEGFA expression to drive angiogenesis. This perfectly fits the definition of synergy, further demonstrating that GM-CSF and IL-1α secreted by CPS synergistically promote angiogenesis in burn wounds. It also suggests that the therapeutic efficacy of CPS is not limited to physical coverage, but also involves the active regulation of the local microenvironment via a multifactorial network.

From a mechanistic perspective, GM-CSF binds to GM-CSFR to recruit and activate JAK2 [15], while IL-1α binding to IL-1R similarly triggers the phosphorylation of intracellular JAK2 [18]. Subsequently, activated JAK2 phosphorylates STAT3 and promotes its nuclear translocation. Once in the nucleus, p-STAT3 not only

directly upregulates VEGFA expression to drive angiogenesis [36], but also promotes the transcription of Cyclin D1, c-Myc, and MMP2/9, enhancing the proliferation and migration capabilities of endothelial cells across multiple dimensions [21]. The central hub role of the JAK2/STAT3 pathway in angiogenesis has been validated in numerous studies, such as the pro-angiogenic effect of ginsenoside Rg1 in spinal cord injury [37] and the pro-angiogenic effect of GM-CSF in the chicken chorioallantoic membrane (CAM) [15]. In the present study, we not only demonstrated in vivo that GM-CSF and IL-1α secreted by CPS effectively activate the JAK2/STAT3 pathway in guinea pig burn tissues, but also showed in vitro that the specific JAK2 inhibitor AG490 significantly blocked the CPS-conditioned medium-induced proliferation, migration, and tube formation of HUVECs. Taken together, these results robustly confirm that GM-CSF and IL-1α secreted by CPS synergistically promote angiogenesis in burn wounds by activating the JAK2/STAT3 pathway (**Figure 5**). A deeper mechanistic analysis reveals that although GM-CSF and IL-1α recognize their respective independent upstream receptors (GM-CSFR and IL-1R), their downstream signals ultimately converge on the JAK2/STAT3 axis. This may construct a potent signal amplification loop within endothelial cells, ensuring the sustained and highly efficient upregulation of key effector factors like VEGFA, thereby ultimately driving the formation of neovascular networks in burn wounds.

Conclusion

In this study, we demonstrated that the lower antigenicity of CPS compared with fresh porcine skin. Transplanting CPS promoted angiogenesis in burn wounds of guinea pigs by secreting GM-CSF and IL-1α. In vitro, it was further verified that GM-CSF and IL-1α secreted by CPS promoted the proliferation, invasion, migration, and tube formation of HUVECs via activating the JAK2/STAT3 pathway. This research confirms the promotion effect of CPS on wound healing and provides theoretical support for the application of cryopreserved porcine skin transplantation.

Limitation

The roles of GM-CSF and IL-1α secreted by cryopreserved porcine skin in other aspects of burn wound healing require further investigation. Additionally, other factors are secreted by the cryopreserved porcine skin and their potential contributions to burn wound healing necessitate further study.

Disclosure of conflict of interest

None.

Abbreviations

CPS, cryopreserved porcine skin; HUVECs, human umbilical vein endothelial cells; GM-CSF, granulocyte-macrophage colony-stimulating factor; IL-1α, Interleukin-1 alpha; VEGFA, Vascular endothelial growth factor A; HE, Hematoxylin-eosin; TEM, transmission electron microscope; IHC, Immunohistochemical; EdU, 5-Ethynyl-2'-deoxyuridine; SD, standard deviation; α-Gal, alpha-Galactosidase A; SLA, swine leukocyte antigen.

Address correspondence to: Guodong Song, Departments of Burns and Plastic Surgery & Wound Repair, Jinan Central Hospital, Shandong University, No. 105 Jiefang Road, Lixia District, Jinan 250013, Shandong, China. E-mail: sgd1232023@163.com

References

[1] Jeschke MG, van Baar ME, Choudhry MA, Chung KK, Gibran NS and Logsetty S. Burn injury. Nat Rev Dis Primers 2020; 6: 11.

[2] Carlton M, Voisey J, Parker TJ, Punyadeera C and Cuttle L. A review of potential biomarkers for assessing physical and psychological trauma in paediatric burns. Burns Trauma 2021; 9: tkaa049.

[3] Rowan MP, Cancio LC, Elster EA, Burmeister DM, Rose LF, Natesan S, Chan RK, Christy RJ and Chung KK. Burn wound healing and treatment: review and advancements. Crit Care 2015; 19: 243.

[4] Chouhan D, Dey N, Bhardwaj N and Mandal BB. Emerging and innovative approaches for wound healing and skin regeneration: current status and advances. Biomaterials 2019; 216: 119267.

[5] Kalsi R, Messner F and Brandacher G. Skin xenotransplantation: technological advances and future directions. Curr Opin Organ Transplant 2020; 25: 464-476.

[6] Zhang L, Xu G, Wei Y, Yuan M, Li Y, Yin M, Chen C, Huang G, Shu B and Wu J. In situ scarless skin healing of a severe human burn wound induced by a hCTLA4Ig gene-transferred por-

cine skin graft. Int J Med Sci 2022; 19: 952-964.
[7] Chiarini A, Dal Pra I and Armato U. In vitro and in vivo characteristics of frozen/thawed neonatal pig split-skin strips: a novel biologically active dressing for areas of severe, acute or chronic skin loss. Int J Mol Med 2007; 19: 245-55.
[8] Ju X, Zhu Z and Li C. Viability and antigenic changes in the skin after preservation under different temperatures. Zhonghua Zheng Xing Shao Shang Wai Ke Za Zhi 1995; 11: 436-9.
[9] Holzer PW, Leonard DA, Shanmugarajah K, Moulton KN, Ng ZY, Cetrulo CL Jr. and Sachs DH. A comparative examination of the clinical outcome and histological appearance of cryopreserved and fresh split-thickness skin grafts. J Burn Care Res 2017; 38: e55-e61.
[10] De Luca M, Albanese E, Bondanza S, Megna M, Ugozzoli L, Molina F, Cancedda R, Santi PL, Bormioli M and Stella M. Multicentre experience in the treatment of burns with autologous and allogenic cultured epithelium, fresh or preserved in a frozen state. Burns 1989; 15: 303-9.
[11] Muller F E. Experience with deep-frozen fresh pig skin in the treatment of 100 burn injury patients. Z Plast Chir 1979; 3: 129-37.
[12] Veith AP, Henderson K, Spencer A, Sligar AD and Baker AB. Therapeutic strategies for enhancing angiogenesis in wound healing. Adv Drug Deliv Rev 2019; 146: 97-125.
[13] Li H, Cao X, Gu X, Dong M, Huang L, Mao C, Xia S, Yang H, Bao X, Yang Y and Xu Y. GM-CSF promotes the development of dysfunctional vascular networks in moyamoya disease. Neurosci Bull 2024; 40: 451-465.
[14] Zhao J, Chen L, Shu B, Tang J, Zhang L, Xie J, Qi S and Xu Y. Granulocyte/macrophage colony-stimulating factor influences angiogenesis by regulating the coordinated expression of VEGF and the Ang/Tie system. PLoS One 2014; 9: e92691.
[15] Valdembri D, Serini G, Vacca A, Ribatti D and Bussolino F. In vivo activation of JAK2/STAT-3 pathway during angiogenesis induced by GM-CSF. FASEB J 2002; 16: 225-7.
[16] Fahey E and Doyle SL. IL-1 family cytokine regulation of vascular permeability and angiogenesis. Front Immunol 2019; 10: 1426.
[17] Salmeron K, Aihara T, Redondo-Castro E, Pinteaux E and Bix G. IL-1alpha induces angiogenesis in brain endothelial cells in vitro: implications for brain angiogenesis after acute injury. J Neurochem 2016; 136: 573-80.
[18] Song Z, Wu W, Wei W, Xiao W, Lei M, Cai KQ, Huang DW, Jeong S, Zhang JP, Wang H, Kadin ME, Waldmann TA, Staudt LM, Nakagawa M and Yang Y. Analysis and therapeutic targeting of the IL-1R pathway in anaplastic large cell lymphoma. Blood 2023; 142: 1297-1311.
[19] Xue C, Xie J, Zhao D, Lin S, Zhou T, Shi S, Shao X, Lin Y, Zhu B and Cai X. The JAK/STAT3 signalling pathway regulated angiogenesis in an endothelial cell/adipose-derived stromal cell coculture, 3D gel model. Cell prolif 2017; 50: e12307.
[20] Xu X, Shi Y, Luan P, Kou W, Li B, Zhai M, You S, Yu Q, Zhuang J, Jian W, Feinberg MW and Peng W. The subcellular redistribution of NLRC5 promotes angiogenesis via interacting with STAT3 in endothelial cells. Theranostics 2021; 11: 4483-4501.
[21] Wu Y, Tian L, Xu Y, Zhang M, Xiang S, Zhao J and Wang Z. CXCR7 silencing inhibits the migration and invasion of human tumor endothelial cells derived from hepatocellular carcinoma by suppressing STAT3. Mol Med Rep 2018; 18: 1644-1650.
[22] Yoshida K. Comparison of low and high doses of pentobarbital or thiopental for euthanasia of isoflurane-anesthetized pigs. J Am Assoc Lab Anim Sci 2023; 62: 185-188.
[23] Shao A, Ling Y, Xu L, Liu S, Fan C, Wang Z, Xu B and Wang C. Xenogeneic bone matrix immune risk assessment using GGTA1 knockout mice. Artif Cells Nanomed Biotechnol 2018; 46 Suppl 3: S359-S369.
[24] Hara H, Koike N, Long C, Piluek J, Roh DS, SundarRaj N, Funderburgh JL, Mizuguchi Y, Isse K, Phelps CJ, Ball SF, Ayares DL and Cooper DK. Initial in vitro investigation of the human immune response to corneal cells from genetically engineered pigs. Invest Ophthalmol Vis Sci 2011; 52: 5278-86.
[25] Zilberman M, Egozi D, Shemesh M, Keren A, Mazor E, Baranes-Zeevi M, Goldstein N, Berdicevsky I, Gilhar A and Ullmann Y. Hybrid wound dressings with controlled release of antibiotics: structure-release profile effects and in vivo study in a guinea pig burn model. Acta biomaterialia 2015; 22: 155-63.
[26] Salvo J, Sandoval C, Schencke C, Acevedo F and Del Sol M. Healing effect of a nano-functionalized medical-grade honey for the treatment of infected wounds. Pharmaceutics 2023; 15: 2187.
[27] McNamee EN, Biette KA, Hammer J, Harris R, Miyazawa H, Lee JJ, Furuta GT and Masterson JC. Targeting granulocyte-macrophage colony-stimulating factor in epithelial and vascular remodeling in experimental eosinophilic esophagitis. Allergy 2017; 72: 1232-1242.
[28] Zhou X, Liu Y, Shen Y, Chen L, Hu W, Yan Y, Feng B, Xiang L, Zhu Y, Jiang C, Dai Z, Huang X, Wu L, Liu T, Fu L, Duan C, Shen S, Li J and Zhang H. Rescue of cardiac dysfunction during chemotherapy in acute myeloid leukaemia by

blocking IL-1alpha. Eur Heart J 2024; 45: 2235-2250.
[29] Tsai CC, Tey SL, Lee MC, Liu CW, Su YT and Huang SC. Mechanism of resveratrol-induced relaxation of the guinea pig fundus. Phytomedicine 2018; 43: 55-59.
[30] Qiu L, Xing D, Zhu Y, Zhuang Z, Sun Y, Gong P and Chen X. Study on the mechanism of no. 8 burn ointment in burn treatment based on network pharmacology and experimental verification. Frontiers in pharmacology 2025; 16: 1511741.
[31] Wu D, Zhao XS, Zhao HF, Xie JH, Wei HJ and Zhu NW. New hope for the treatment of severe skin injury: genetically engineered porcine skin xenotransplantation. Xenotransplantation 2025; 32: e70057.
[32] Young JB, Gondek SP, Troche M, Summitt JB, Rae L, Thayer WP and Kahn SA. The use of porcine xenografts in patients with toxic epidermal necrolysis. Burns 2016; 42: 1728-1733.
[33] Yamamoto T, Iwase H, King TW, Hara H and Cooper DKC. Skin xenotransplantation: historical review and clinical potential. Burns 2018; 44: 1738-1749.
[34] Haller HL, Blome-Eberwein SE, Branski LK, Carson JS, Crombie RE, Hickerson WL, Kamolz LP, King BT, Nischwitz SP, Popp D, Shupp JW and Wolf SE. Porcine xenograft and epidermal fully synthetic skin substitutes in the treatment of partial-thickness burns: a literature review. Medicina (Kaunas) 2021; 57: 432.
[35] Huang HW, Chen CY, Huang YH, Yeh CT, Wang CS, Chang CC and Lin KH. CMAHP promotes metastasis by reducing ubiquitination of Snail and inducing angiogenesis via GM-CSF overexpression in gastric cancer. Oncogene 2022; 41: 159-172.
[36] Ma Q, Wang H, Zhao X, Gao X, Zhang Q, Liu Y, Ji Y, Sun Y, Lei K and Luo W. AURKA promotes angiogenesis in uveal melanoma via activation of the JAK2/STAT3/VEGFA signaling pathway. Cancer Cell Int 2025; 25: 207.
[37] Yin S, Xia F, Zou W, Jiang F, Shen K, Sun B and Lu Z. Ginsenoside Rg1 regulates astrocytes to promote angiogenesis in spinal cord injury via the JAK2/STAT3 signaling pathway. J Ethnopharmacol 2024; 334: 118531.